J Membrane Biol (2009) 229:19–25
DOI 10.1007/s00232-009-9172-6

Alterations of the Plasma Membrane Caused by Murine Polyomavirus Proliferation: An Electrorotation Study

Valerio Berardi · Cecilia Aiello · Adalberto Bonincontro · Gianfranco Risuleo

Received: 2 March 2009 / Accepted: 17 April 2009 / Published online: 9 May 2009

Abstract In this report we investigate the alterations of the dielectric properties of the plasma membrane caused by the infection of cultured fibroblasts with murine polyomavirus. The approach consists in a well-established dielectric spectroscopy technique, electrorotation, which has been successfully used in our laboratory to study the alterations of the plasma membrane of cells exposed to various forms of stress. The response to viral proliferation was time dependent as shown by evaluation of the de novo synthesis of viral DNA. This response was paralleled by gradual damage of the membrane evidenced by alteration of the dielectric parameters, specific capacitance and conductance. The electrorotation results show a reduced effect on the dielectric properties of the membrane when infection is carried out in the presence of a natural oil (MEX). In this case a drastic reduction in viral DNA synthesis was also monitored, thus indicating an antiviral action of this product.

Keywords Polyomavirus infection · Dose/response effect · Electrorotation · Membrane structure/function

V. Berardi · C. Aiello · G. Risuleo (✉)
Dipartimento di Genetica e Biologia Molecolare, Università di Roma "La Sapienza", p.le A. Moro 5, Rome 00185, Italy
e-mail: gianfranco.risuleo@uniroma1.it

A. Bonincontro
CNISM-Dipartimento di Fisica, Università di Roma "La Sapienza", p.le A. Moro 5, Rome 00185, Italy

A. Bonincontro · G. Risuleo
SOFT-INFM-CNR Research Centre, Università di Roma "La Sapienza", p.le A. Moro 5, Rome 00185, Italy

Introduction

Murine polyomavirus (Py) is an extremely well-characterized model system used to investigate a variety of biological phenomena. The virus genome is formed by a small double-stranded circular DNA molecule and has been "historically" considered a good model of the eukaryotic chromosome. Polyomavirus relies completely on the metabolic machinery of the infected cell, and therefore it has been used to investigate cellular and molecular functions such as DNA replication and regulation of RNA transcription and translation as well as mechanisms of tumor transformation. Like other polyomaviruses, Py can very efficiently transform nonpermissive cells in culture. In addition, these viruses are able to cause tumors if injected in immunosuppressed or singeneic animals. The "classical" book edited by Tooze (1982) possibly still represents the most complete work on this subject. However, although reports exist documenting the presence of Py DNA sequences in human tumor tissues (see, e.g., Casini et al. 2005; Muñoz-Mármol et al. 2006; Giuliani et al. 2007; Shiramizu et al. 2007), the actual role of these viruses as causative agents of tumor transformation within the immunocompetent population is still strongly debated (see, e.g., Barbanti-Brodano et al. 2006; Eash et al. 2006; Moens et al. 2007). Finally, in our laboratory Py has also been used to test the cytotoxic and/or antiviral potential of substances of natural origin (Iacoangeli et al. 2000; Campanella et al. 2002; Di Ilio et al. 2006).

A particular aspect of productive infection with Py is represented by the entry of the virion into the cell and by its interaction with the plasma membrane. However, the mechanisms of virion entry through the membrane and its transport to the nucleus, where it is uncoated prior to initiation of proliferation, are not yet fully understood. In

the case of Py, it is known that the main capsid protein VP1 binds sialic acid residues, while the homologous protein of SV40 binds membrane gangliosides (Stehle et al. 1994; Tsai et al. 2003). It is commonly accepted that these viruses are internalized through caveolin-dependent or -independent pathways and are subsequently transferred to the endoplasmic reticulum (ER) system (Gilbert and Benjamin 2000; Pelkmans et al. 2001). With respect to this, it was recently published that the ER-specific protein Derlin-2 is required for productive entry and initiation of Py infection (Lilley et al. 2006). Also, the dynamics of internalization and the impact on the infected cell physiology have recently been reviewed (Damm and Pelkmans 2006). However, information on possible membrane damage consequent to virus penetration into the cell is not very abundant, even though reports have been published on the mode and effects of viral proliferation on the plasma membrane (Norkin 1977; Bonincontro et al. 1996; Drachenberg et al. 2003; Damm et al. 2005).

This report focuses on the structural/functional alterations of the plasma membrane consequent to viral infection. The study was conducted using the spectroscopic technique known as electrorotation (Arnold and Zimmermann 1982; Mischel et al. 1982; Gimsa et al. 1991; Bonincontro et al. 1997; Gimsa 2001; Cen et al. 2004). This powerful technique allows single-cell examination and, thus, evaluation of the dielectric parameters of the plasma membrane: specific capacitance (C) and specific conductance (G). The alteration of these parameters is suggestive of a change in plasma membrane structure and/or function. Evidence is presented that these alterations of the dielectric properties are virus induced.

Materials and Methods

Cell Cultures, Viral Infection, and DNA Replication Assays

Cultures of murine fibroblasts (3T6 cell line) were routinely maintained at 37°C in a 5% carbon dioxide atmosphere in DMEM supplemented with 10% newborn serum, glutamine (50 mM f.c.), and penicillin-streptomycin (10^3 U/ml each). Viral infection was performed at 4 pfu × cell for 2 h at 37°C with shaking. Infection procedure and de novo synthesized DNA assays (replication assays) have been described in detail in previous work (see, e.g., Campanella et al. 2002; Pastore et al. 2004). Viral DNA was visualized after agarose gel electrophoresis in the presence of ethidium bromide (0.5 μg/ml, final concentration).

Whole Neem oil was supplied by Trifoglio-MR GmgH (Lahnau, Germany). Methanolic extract (MEX) was obtained by six consecutive methanol extractions (twice the volume of the whole oil each time). The extract was subsequently freeze-dried in vacuo and the pellet thus obtained was dissolved in ethanol in a stock solution at a concentration of 100 mg/ml: for details on the procedure see Di Ilio et al. (2006).

Electrorotation Apparatus

A standard apparatus for electrorotation was used. The frequency range used in each experiment was 100 Hz–500 kHz. In this interval it is possible to monitor only relaxation at the interface of solvent/plasma membrane.

The rotating electrical field was generated by superimposing four square waves out of phase by 90°. The square pulses were applied to the copper miniplate electrodes of the measuring cell, which form a central circular cavity with a volume of about 10 μl. The whole setup was mounted on a microscope glass slide. The rotating cells were observed via a monitor and at each session the rotation period of 20 cells was considered (for further details on measurements and caveats see Bonincontro et al. 2007).

Statistical Treatment of Experimental Data

All experiments were performed in triplicate. Error bars indicate the standard error of the mean (±SE).

Results and Discussion

Electrorotation Theory

An electric field applied to a polydisperse cell suspension induces a dipole moment. This is due to the charges compartmentalized at the interface between cell membrane and solvent. When this interfacial polarization relaxes, the induced dipole moment undergoes a phase shift with respect to the electric field. This causes a torque moment and cells begin to rotate. The period depends on the frequency of the applied field according to the formula, based on the so-called single-shell model:

$$T(f) = T_{\min} \frac{1 + \left(\frac{f}{f*}\right)^2}{2\left(\frac{f}{f*}\right)} \quad (1)$$

where f is the frequency of the applied field, f^* is the relaxation frequency, and $T_{\min}$ is the value of the rotation period at the relaxation frequency. The value of f^* depends on the solvent conductivity following the formula:

$$f* = \frac{1}{2\pi rc}\left[\frac{1}{\frac{1}{\sigma_e}+\frac{1}{\sigma_i}} + rG\right] \quad (2)$$

where C and G are, respectively, the specific capacitance and conductance of the cell plasma membrane with radius r, σ_e is the solvent conductivity, and σ_i is the conductivity of the cytoplasm considered to be homogeneous. Since $\sigma_e << \sigma_i$, Eq. 2 becomes

$$f* = \left(\frac{1}{\pi r \quad C}\right)\sigma_e + \left(\frac{1}{2\pi \quad C}\right)G \quad (3)$$

The electrorotation theory is illustrated in detail in the literature (Arnold and Zimmermann 1982; Mischel et al. 1982; Gimsa et al. 1991; Gimsa 2001).

Dielectric Parameters of the Plasma Membrane After Py Infection

As an example of a typical experimental result, Fig. 1 (top panel) shows the average rotation period as a function of different rotating field frequencies in control cells. The experimental data were fitted according to Eq. 1 and the relaxation frequency was determined. Measurements were done at different conductivities of the solvent (0.5, 1.0, and 1.5 mM NaCl; only the curve at 0 mM NaCl is shown). The relaxation frequencies $f*$ are reported as a function of the solvent conductivity, and as expected from Eq. 3, they form a straight line (Fig. 1 bottom panel). The average cell radius was estimated for a statistically significant number of cells and its value was 8.5 ± 0.5 μm. We subsequently calculated the dielectric parameters C and G. An analogous procedure was adopted for cells infected with Py at various times of infection (we would like to point out that the cell radius did not show a significant difference in infected cells versus control cells). Table 1 summarizes the dielectric parameters obtained for controls and infected cells. These data suggest that a correlation exists between infection time, i.e., viral proliferation, and alteration of the plasma membrane.

The actual progression of the viral infection was monitored by analysis of the de novo synthesis of viral progeny DNA. Figures 2, 3, 4, 5 report the electropheretograms (panels at the right), which show a steady increase in viral DNA production as infection time proceeds; this is summarized and quantified in Fig. 6. The panels at the left show the straight line reporting the relaxation frequencies $f*$ as a function of the solvent conductivity. From these data the variations of C and G values may calculated. Data reported in Table 1 show that the infection causes an increasing trend in the C value, while a significant rise in G is monitored only at a prolonged infection time. The modest increase in G at a shorter time of infection is in agreement with the fact that viral DNA production reaches its maximum at about 40 h postinfection as reported in literature. The parameter C is strongly related to the membrane structural properties: therefore one can conclude that the virus entry across the plasma membrane causes only a modest structural rearrangement. The variations in C

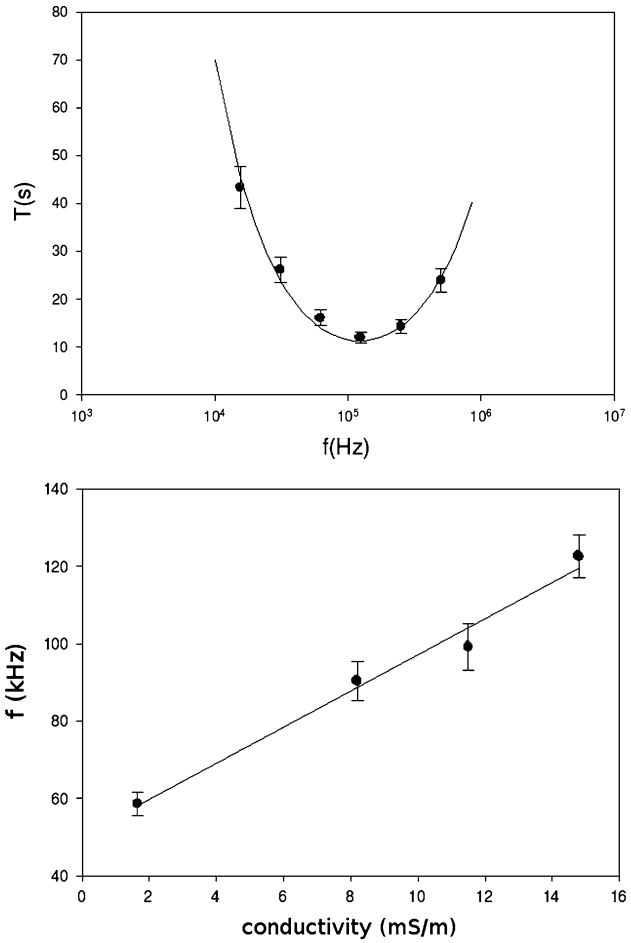

Fig. 1 *Top* Average rotation period as a function of rotating field frequency in untreated control cells. The solvent was salt-free 0.3 M sucrose. The *curve* is the result of the best fit according to Eq. 1. *Bottom* Relaxation frequency $f*$ as a function of solvent conductivity. The *straight line* results from the best fit according to Eq. 3. *Error bars* indicate ±SE

Table 1 Dielectric parameters of the plasma membrane at different times of infection with murine polyomavirus

Time of infection	Specific capacitance C (μF/cm^2)	Specific conductance G (S/cm^2)
Mock infection	0.8 ± 0.1	0.26 ± 0.06
24 h	0.9 ± 0.1	0.20 ± 0.04
48 h	1.2 ± 0.2	0.25 ± 0.04
72 h	1.3 ± 0.2	0.45 ± 0.03

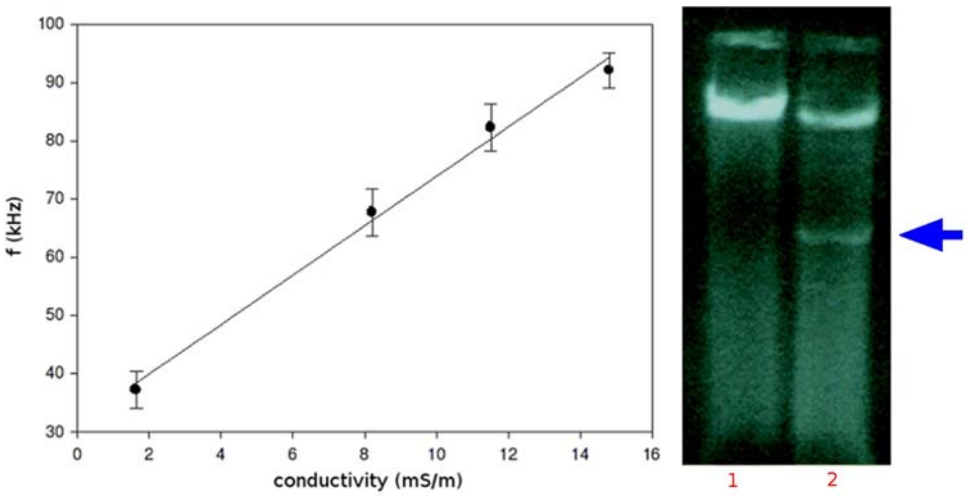

Fig. 2 *Left* Relaxation frequency f^* as a function of solvent conductivity. The *straight line* results from the best fit according to Eq. 3. *Right* Lane 1, electropheretogram obtained from mock-infected control cells; lane 2, progeny viral DNA yield at 24 h postinfection, indicated by the *arrow*. The *upper band* is high molecular weight chromosomal DNA, a normal contaminant in this extraction protocol. *Error bars* indicate ±SE

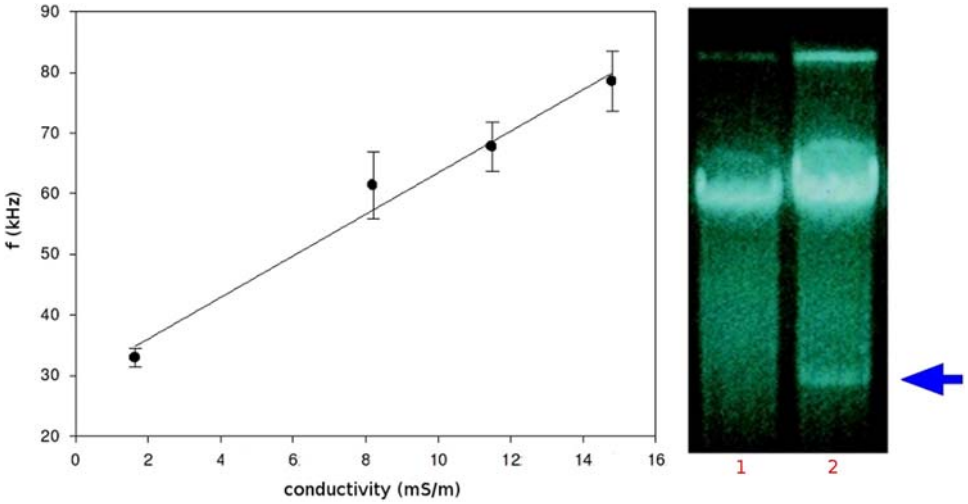

Fig. 3 *Left* Relaxation frequency f^* as a function of solvent conductivity. The *straight line* results from the best fit according to Eq. 3. *Right* Lane 1, electropheretogram obtained from mock-infected control cells; lane 2, progeny viral DNA yield at 48 h postinfection, indicated by the *arrow*. *Error bars* indicate ±SE

values are, within the measurement error, rather limited. On the other hand, the increase in G, a parameter related to membrane ion permeability, may suggest that a correlation exists between viral DNA synthesis and an overall stimulation of cell functions.

Electrorotation Measurements After Inhibition of Viral DNA Production

To correlate the variation of the dielectric parameters with viral DNA synthesis, we performed a new set of measurements on cell samples infected with Py in the presence of MEX. This natural complex mixture shows a variety of biological activities, among which is an antiviral one (Subapriya and Nagini 2005). In previous electrorotation studies performed in our laboratory, MEX was also shown to alter membrane fluidity after administration to cultured cells (Bonincontro et al. 2007). In any case the membrane is one of the main targets of this natural mixture (Ricci et al. 2008). The results of these new dielectric measurements are reported in Table 2 and in Fig. 6, which summarizes the evaluation of viral DNA production after treatment with MEX. In the presence of MEX, the parameter C remains unaltered and the increasing trend, observed previously, is abolished. This implies that the membrane essentially maintains its structural features, unlike the previous data obtained in the absence of MEX (cf. Tables 1, 2), which may suggest that the viral DNA production is impaired. Figure 2 shows that after 48 h of infection in the presence of MEX, viral DNA synthesis decreases dramatically. Last but not least, these results show that MEX actually has an antiviral action toward Py proliferation: this activity needs further elucidation and experimental work is in progress in our laboratory. Only the data at 48 h postinfection are shown, since at longer infection times, electrorotational data become unreliable.

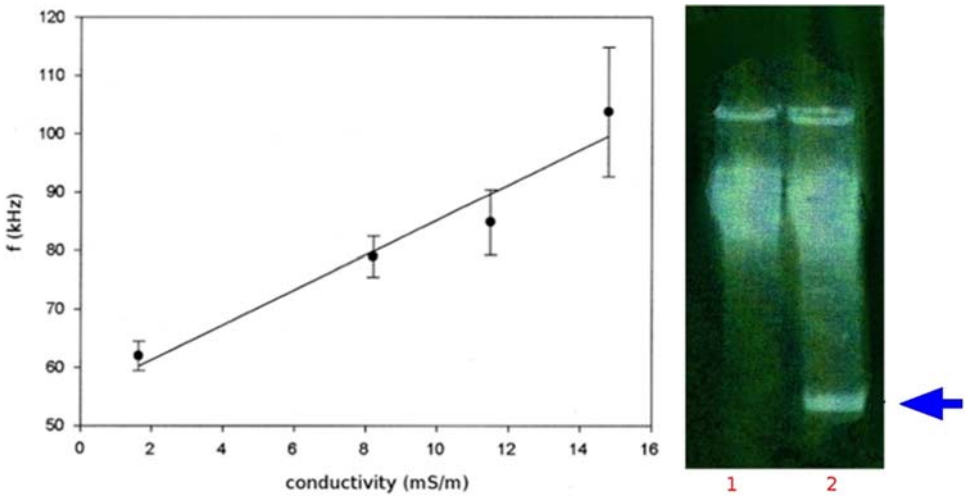

Fig. 4 *Left* Relaxation frequency *f** as a function of solvent conductivity. The *straight line* results from the best fit according to Eq. 3. *Right* Lane 1, electropheretogram obtained from mock-infected control cells; lane 2, progeny viral DNA yield at 72 h postinfection, indicated by the *arrow*. *Error bars* indicate ±SE

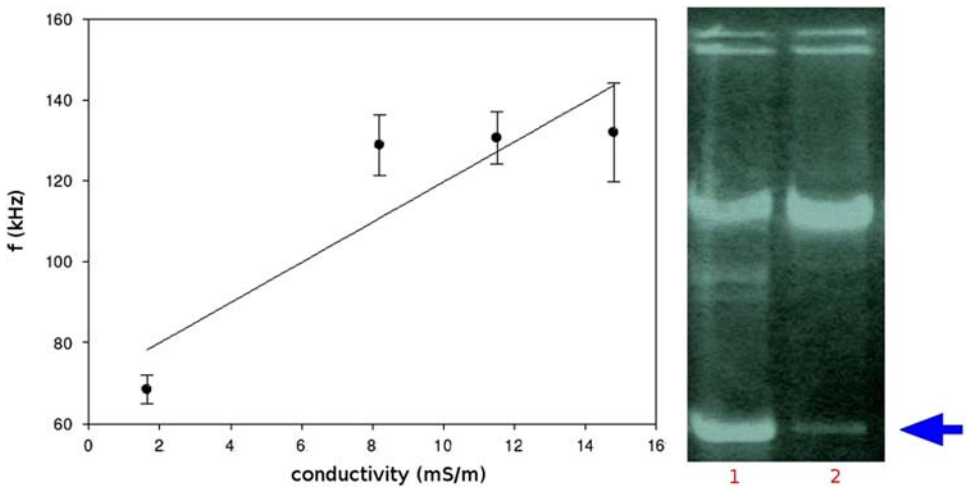

Fig. 5 *Left* Relaxation frequency *f** as a function of solvent conductivity. The *straight line* results from the best fit according to Eq. 3. *Right* Lane 1, electropheretogram obtained from mock-infected control cells; lane 2, progeny viral DNA yield at 48 h postinfection, indicated by the *arrow*, but in this case infection was done in the presence of MEX (5 mg/mL, final concentration). Data at 72 h are not shown since the toxicity of MEX is too elevated at this time; see the text. *Error bars* indicate ±SE

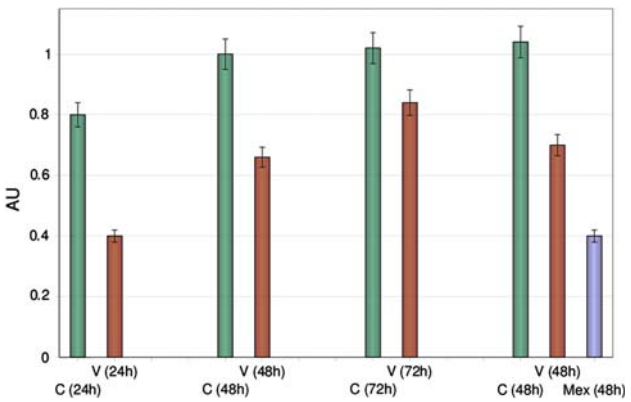

Fig. 6 Summary of the progeny viral DNA yield at various times postinfection. *Green bars*: mock-infected control cells. *Red bars*: viral DNA. *Blue bar*: viral DNA obtained in the presence of MEX. *Error bars* indicate ±SE (color figure online)

Table 2 Dielectric parameters of the plasma membrane at different times of infection with murine polyomavirus in the presence of the Neem derivative MEX

Time of infection	Specific capacitance C (μF/cm^2)	Specific conductance G (S/cm^2)
Mock infection	0.8 ± 0.1	0.26 ± 0.06
24 h	0.9 ± 0.2	0.29 ± 0.08
48 h	0.8 ± 0.2	0.34 ± 0.06

Note: Data at 72 h are omitted since, after this time of infection, MEX is too toxic to provide reliable data

This is because, after such a long exposure to MEX, the cytotoxic effect on the cells and the nonhomogeneity of the cell population (infected vs. uninfected, different stages of virus proliferation) cannot be neglected (Bonincontro et al. 2007).

In summary, the lower increase in parameter *G*, compared to the results obtained in the absence of MEX, should be attributed to a direct effect mediated by MEX rather than to viral DNA synthesis (Bonincontro et al. 2007; Ricci et al. 2008). In any case, it is worth noting that the electrorotational data presented here are in very good agreement with results obtained in our laboratory using an impedance methodology (Bonincontro et al. 1996).

Conclusion

The results obtained in this work corroborate the idea that dielectric spectroscopy is a good tool to investigate the structure/function relationships of the plasma membrane. Also, this work shows that infection with Py has little effect on the structural properties of the cell membrane, while membrane permeability seems to increase significantly. In infection experiments carried out in the presence of a natural mixture known as MEX the structural damage was eliminated. However, the presence of MEX induces per se an increase in ion permeability, masking and/or eliminating a possible effect of the viral proliferation. In light of these data an antiviral action of MEX is suggested, and this deserves further investigation.

Acknowledgments This work was in partial fulfillment of the Ph.D. thesis of V.B. Funding by the Italian Ministry of Education (MIUR) is acknowledged.

References

Arnold WM, Zimmermann U (1982) Rotating-field-induced rotation and measurement of the membrane capacitance of single mesophyll cells of *Avena sativa*. Z Nat Forsch C 37:908–915

Barbanti-Brodano G, Sabbioni S, Martini F, Negrini M, Corallini A, Tognon M (2006) BK virus, JC virus and simian virus 40 infection in humans, and association with human tumors. Adv Exp Med Biol 577:319–341

Bonincontro A, Iacoangeli A, Risuleo G (1996) Electrical conductivity dispersion as a probe of membrane function after murine polyomavirus infection in cells in culture. Biosci Rep 16:41–48

Bonincontro A, Iacoangeli A, Melucci-Vigo G, Risuleo G (1997) Apoptosis dependent decrease of the inter-membrane ion traffic in cultured mouse fibroblasts shown by conductivity dispersion. Biosci Rep 17:547–556

Bonincontro A, Di Ilio V, Pedata O, Risuleo G (2007) Dielectric properties of the plasma membrane of cultured murine fibroblasts treated with a non terpenoid extract of *A. indica* seeds. J Membr Biol 215:75–79

Campanella L, Delfini M, Ercole P, Iacoangeli A, Risuleo G (2002) Molecular characterization and action of usnic acid: a drug that inhibits proliferation of mouse polyomavirus in vitro and its main target is RNA transcription. Biochimie 84:234–329

Casini B, Borgese L, Del Nonno F, Galati G, Izzo L, Perrone Donnorso R, Risuleo G, Visca P (2005) Presence and incidence of DNA sequences of human polyomaviruses BKV and JCV in colon-rectal tumor tissues. Anticancer Res 25:1079–1085

Cen EG, Dalton C, Li Y, Adamia S, Pilarski LM, Kaler KV (2004) A combined dielectrophoresis, traveling wave dielectrophoresis and electro-rotation microchip for the manipulation and characterization of human malignant cells. J Microbiol Methods 58:387–401

Damm EM, Pelkmans L (2006) Systems biology of virus entry in mammalian cells. Cell Microbiol 8:1219–1227

Damm EM, Pelkmans L, Kartenbeck J, Mezzacasa A, Kurzchalia T, Helenius A (2005) Clathrin- and caveolin-1-independent endocytosis: entry of simian virus 40 into cells devoid of caveolae. J Cell Biol 168:477–488

Di Ilio V, Pasquariello N, van der Esch AS, Cristofaro M, Scarsella G, Risuleo G (2006) Cytotoxic and antiproliferative effects induced by a non terpenoid polar extract of *A. indica* seeds on 3T6 murine fibroblasts in culture. Mol Cell Biochem 287:69–77

Drachenberg CB, Papadimitriou JC, Wali R, Cubitt CL, Ramos E (2003) BK polyoma virus allograft nephropathy: ultrastructural features from viral cell entry to lysis. Am J Transplant 3:1383–1392

Eash S, Manley K, Gasparovic M, Querbes W, Atwood WJ (2006) The human polyomaviruses. Cell Mol Life Sci 63:865–876

Gilbert JM, Benjamin TL (2000) Early steps of polyomavirus entry into cells. J Virol 74:8582–8588

Gimsa J (2001) A comprehensive approach to electro-orientation, electrodeformation, dielectrophoresis, and electro-rotation of ellipsoidal particles and biological cells. Bioelectrochemistry 54:23–31

Gimsa J, Marszalek P, Loewe U, Tsong TY (1991) Dielectrophoresis and electro-rotation of neurospora slime and murine myeloma cells. Biophys J 60:749–760

Giuliani L, Jaxmar T, Casadio C, Gariglio M, Manna A, D'Antonio D, Syrjanen K, Favalli C, Ciotti M (2007) Detection of oncogenic viruses SV40, BKV, JCV, HCMV, HPV and p53 codon 72 polymorphism in lung carcinoma. Lung Cancer 57:273–281

Iacoangeli A, Melucci-Vigo G, Risuleo G (2000) Mechanism of the inhibition of murine polyomavirus DNA replication induced by the ionophore monensin. Biochimie 82:35–39

Lilley BN, Gilbert JM, Ploegh HL, Benjamin TL (2006) Murine polyomavirus requires the endoplasmic reticulum protein Derlin-2 to initiate infection. J Virol 80:8739–8744

Mischel M, Voss A, Pohl HA (1982) Cellular spin resonance in rotating electric fields. J Biol Phys 10:223–226

Moens U, Van Ghelue M, Johannessen M (2007) Oncogenic potentials of the human polyomavirus regulatory proteins. Cell Mol Life Sci 64:1656–1678

Muñoz-Mármol AM, Mola G, Ruiz-Larroya T, Fernández-Vasalo A, Vela E, Mate JL, Ariza A (2006) Rarity of JC virus DNA sequences and early proteins in human gliomas and medulloblastomas: the controversial role of JC virus in human neurooncogenesis. Neuropathol Appl Neurobiol 32:131–140

Norkin LC (1977) Cell killing by simian virus 40: impairment of membrane formation and function. J Virol 21:872–879

Pastore D, Iacoangeli A, Galati G, Izzo L, Fiori E, Caputo M, Castelli M, Risuleo G (2004) Variations of telomerase activity in cultured mouse fibroblasts upon proliferation of polyomavirus. Anticancer Res 24:791–794

Pelkmans L, Kartenbeck J, Helenius A (2001) Caveolar endocytosis of simian virus 40 reveals a new two-stepvesicular-transport pathway to the ER. Nat Cell Biol 3:473–483

Ricci F, Berardi V, Risuleo G (2008) Differential cytotoxicity of MEX: a component of Neem oil whose action is exerted at the cell membrane level. Molecules 14:122–132

Shiramizu B, Hu N, Frisque RJ, Nerurkar VR (2007) High prevalence of human polyomavirus JC VP1 gene sequences in pediatric malignancies. Cell Mol Biol (Noisy-le-grand) 53:4–12

Stehle T, Yan Y, Benjamin TL, Harrison SC (1994) Structure of murine polyomavirus complexed with an oligosaccharide receptor fragment. Nature 369:160–163

Subapriya R, Nagini S (2005) Medicinal properties of neem leaves: a review. Curr Med Chem Anticancer Agent 5:149–156

Tooze J (ed) (1982) DNA tumor viruses—molecular biology of tumor viruses, 2nd edn. Cold Spring Harbor Laboratory Press, Cold Spring Harbor

Tsai B, Gilbert JM, Stehle T, Lencer W, Benjamin TL, Rapoport TA (2003) Gangliosides are receptors for murine polyoma virus and SV40. EMBO J 22:4346–4355